PROCEEDINGS OF THE ROYAL SOCIETY A MATHEMATICAL, PHYSICAL & ENGINEERING SCIENCES

The Evaporation and Combustion of Levitated Arrays of Two, Three and Five Droplets at a Hot Surface

S. Chandra and C. T. Avedisian

Proc. R. Soc. Lond. A 1988 **418**, doi: 10.1098/rspa.1988.0089, published 9 August 1988

Proc. R. Soc. Lond. A **418**, 365–382 (1988)
Printed in Great Britain

The evaporation and combustion of levitated arrays of two, three and five droplets at a hot surface

By S. Chandra and C. T. Avedisian
Sibley School of Mechanical and Aerospace Engineering, Cornell University, Ithaca, New York 14853, *U.S.A.*

(*Communicated by D. B. Spalding, F.R.S. – Received* 20 *November* 1987)

[Plates 1–4]

The interactions between droplets in several geometrical arrays in Leidenfrost evaporation and combustion on a hot surface were studied. Comparisons between evaporation and burning times of isolated droplets, two- and three-droplet linear arrays, and a five-droplet array (a centre droplet surrounded by four droplets) were made. The liquids studied were water, *n*-heptane, and *n*-hexadecane at 0.101 MPa and at surface temperatures above their respective Leidenfrost values. A range of centre distance to initial droplet diameter ratios, L/d_0, were studied ($2 < L/d_0 < \infty$).

The evaporation or burning rates of droplets in binary arrays were found to be identical to those of isolated droplets ($L/d_0 \to \infty$). The flames around each droplet, however, merged as the droplets were brought closer together. In three- and five-droplet arrays more significant interactions were observed, with the edge droplets in the arrays burning faster than the centre droplets. The results are explained on the basis of flame-height measurements for the arrays. In pure evaporation, though, the droplets evaporated without regard for their neighbours.

Nomenclature

a	horizontal droplet axis
b	vertical droplet axis
C	constant, defined in (5b)
d	equivalent droplet diameter
d_0	initial equivalent droplet diameter
F_{df}	radiation shape factor
g	acceleration due to gravity
h	convective heat transfer coefficient
H_i	height of flame surrounding an array of i drops
k	combusion rate
k_g	conductivity of gas around droplets
L	droplet centre-to-centre spacing
Nu_i	Nusselt number for convective heat transfer to a droplet in an array of i drops
Pr	Prandtl number

q_{fi} Convective heat flux to a droplet from the flame around an array of i drops
q_{ti} $q_{fi}+q_w+q_{rad}$
q_{rad} radiative heat flux to a droplet from the flame
q_w heat flux from the surface to a droplet by conduction through the vapour film
t time
T_a ambient temperature
T_d droplet temperature
T_f flame temperature
T_w surface temperature
ΔT temperature difference T_f-T_a
β thermal-expansion coefficient
δ thickness of vapour film under droplet
ν kinematic viscosity
σ Stefan–Boltzmann constant

1. Introduction

The interaction between droplets in a spray causes them to behave differently than isolated droplets. As such, experiments performed on isolated droplets may not be relevant to droplets in close proximity to other droplets. For example, prior work on the combustion of binary-droplet arrays in an unbounded ambience, that is *far* from surfaces, has revealed that the burning rate, evolution of droplet diameter, and flame shape of droplets in the array are generally different than a corresponding isolated droplet (Rex *et al.* 1956; Fedoseeva 1972; Brzustowski *et al.* 1979; Miyasaka & Law 1981; Xiong *et al.* 1984).

Additional complications arising from droplet–wall interactions created by collisions of the droplets in a spray with the confinement walls can make it even more tenuous to judge how droplets in a spray which impact a hot surface behave from studies of isolated droplets. If the temperature of the surface is greater than the so-called Leidenfrost temperature, the pressure of the vapour escaping beneath the droplet will be sufficient to levitate the droplet above the surface rather like a hovercraft. Interest in this problem extends to such applications as combustion of fuel sprays in confined geometries, cooling of hot electronic devices with a liquid spray, and fire extinguishment of burning materials. Accordingly, whereas several experimental studies have been performed to understand droplet–wall interactions above the Leidenfrost point, all of this work has concerned *isolated* droplets. Much of the early work on this problem has been reviewed by Gottfried *et al.* (1966); effects of the surface temperature (Gottfried & Bell 1966), surface material and roughness (Baumeister & Simon 1973), surface porosity (Avedisian & Koplik 1987), droplet volume (Gottfried *et al.* 1966) and ambient pressure (Emmerson 1975) on droplet evaporation as well as the ignition and combustion of isolated droplets (Tamura & Tanasawa 1959; Temple-Pediani 1969) have been studied.

This work was undertaken to study experimentally the evaporation and

burning of droplet arrays on a hot surface above the Leidenfrost point. The intent was to obtain a realistic view of how droplets evaporate and burn at hot surfaces when they are close to other droplets, but not at the expense of revealing the fundamental mechanisms governing any possible interactions between the droplets. To this end an experiment was designed to hold captive up to five droplets on a hot horizontal surface and to observe by photographic means their evaporation and burning histories. The effect of spacing and arrangements of droplets on the evaporation time, evolution of droplet diameter, Leidenfrost temperature, and flame shape were studied. Four configurations of droplets were studied as shown in figure 1: a single droplet; two droplets, which is the simplest case of droplet interaction; a three-droplet linear array, which is the simplest three-droplet configuration in which one of the droplets (the centre one in the array) is between two other droplets (as contrasted with a triangular matrix); and five droplets, which is probably the most elementary matrix of a droplet in a spray surrounded on all sides. Results from such elementary configurations may still be pertinent to the more complex problem of irregular droplet arrays such as might be produced by impact of droplets in a spray with a hot surface. It is clear that the more complicated problem should be addressed in a fundamental manner in a first study, and from this perspective emerged the present approach.

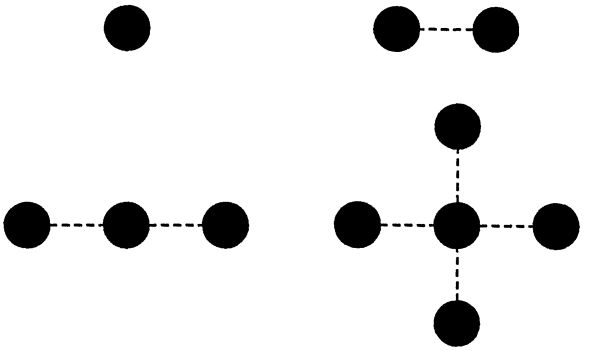

FIGURE 1. Arrays studied (top view).

The fluids used were water, *n*-heptane (C_7H_{16}) and *n*-hexadecane ($C_{16}H_{34}$). To isolate the effects of droplet configuration, the following were held constant: initial droplet volume 0.013 ml for heptane, 0.015 ml for hexadecane and 0.031 ml for water), ambient pressure (0.101 MPa), ambient temperature (*ca.* 295 K) and surface material (polished stainless steel). The surface temperatures ranged from 150 °C to 450 °C (water), 200 °C to 400 °C (heptane) and 390 °C to 550 °C (hexadecane). Observations were made both above and below the Leidenfrost temperature for water, whereas the minimum surface temperatures studied for heptane and hexadecane were above their Leidenfrost points.

For binary-droplet arrays three droplet centre-to-centre distances (L) were examined: 6 mm, 9 mm and 12 mm. For three- and five-droplet arrays only a 6 mm spacing was considered. At the smallest spacing (6 mm) the circumference-to-

circumference distance was about 2 mm. For Leidenfrost drops, these spacings were considered to be the smallest useful working distance to avoid the droplets colliding and coalescing during evaporation because of their periodic movement on the surface. This lower limit was also selected on the belief that a single flame would surround both droplets. This conjecture was based on reference to prior work for burning of binary droplet arrays in an *unbounded* ambience. The phenomenon of flame separation could then be addressed as L/d_0 was increased.

2. Apparatus

The experimental method consisted of simultaneously depositing the droplets, either singly or in regular geometric arrays (e.g. figure 1), on a horizontal surface, and then recording their evaporative behaviour by photographic means. To restrict lateral movement of the droplets, conical depressions were machined on the surface with centres at the desired interdroplet spacings. The droplets were placed in the centres of these depressions. Figure 2 is a schematic diagram of the apparatus. Principal components were: a heating unit; droplet injector; a removable polished stainless steel test surface containing the surface depressions

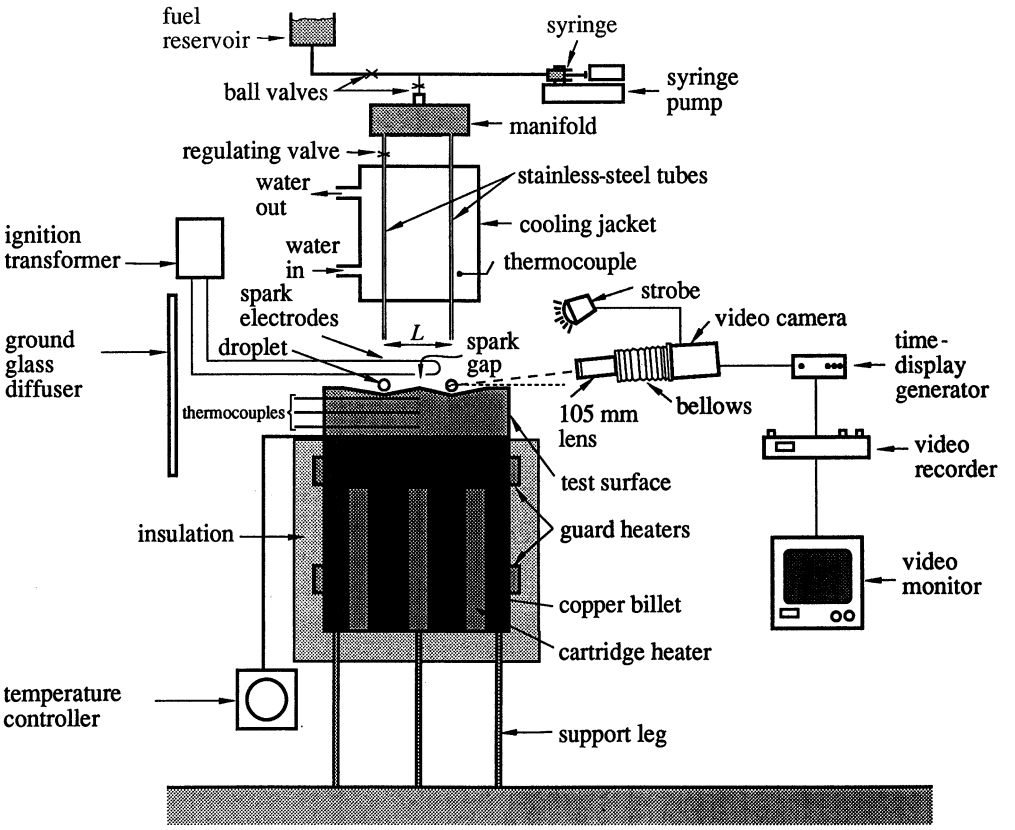

Figure 2. Schematic diagram of apparatus.

and photographic instruments to record flame shape and instantaneous droplet diameters.

The heater block was a cylindrical copper billet (76.2 mm diameter and 127 mm long) containing five symmetrically placed cartridge heaters (Hotwatt cat. no. HS374). The surface temperature could be controlled with an Omega E924K analogue temperature controller that regulated the voltage to the heaters.

The droplet injector consisted of a brass manifold to which were attached five stainless steel tubes, 1.65 mm in diameter. Each tube was connected to a needle valve which permitted individual control of the flow rate through the tube. A brass spacer ensured that the distance between the ends of the tubes was the same as the centre-to-centre distance of the depressions in the surface being studied. Figures 3 and 4, plate 1, show the design of the injector.

Liquid was forced through the injector tubes by means of a Sage Instruments model 341 A syringe pump at a flow rate of 1.7 ml min^{-1}; low enough to allow a droplet to form at the end of an injector tube and to detach under its own weight. The independent control of the flow rate through each tube allowed adjustment of the time difference between detachment of drops from the tubes to less than 0.1 s for two drops and 0.3 s for simultaneous generation of five drops. The ends of the tubes were held directly above the centres of the indentations in the surface at a height of approximately 5 mm. After deposition of the droplets, the injector was moved aside so that it was no longer directly above the test surface. This was done to avoid interference of the injector tubes with the flames around the drops.

The test surfaces were 13 mm thick by 76.2 mm diameter polished stainless steel. Four such surfaces were made, on each of which were machined conical indentations at the desired centre-to-centre spacings. An infinite spacing corresponded to only one drop on the surface. The centres of the depressions were maintained at a depth of 0.2 mm (the angle of indentation varied from 2° to 4° depending on the centre-to-centre distance) which was sufficient to restrict lateral movement of the droplets and to minimize any tendency of the drops to coalesce. It is noted that if droplets smaller than 0.2 mm in diameter rest at the centre of the depression, they would be completely shielded from neighbouring drops by the projected vertical wall of the conical indentation; droplets of this size existed only during the last 2% of the droplet lifetime for the initial droplet sizes studied. However, such shielding was probably minimal because it was observed that as the droplets became smaller, their average levitation height increased, reaching approximately 1 mm towards the end of the droplet lifetime. This height was sufficient to lift the droplet well above the depression and to bring it in view of its neighbours.

Figure 5, plate 2, shows a series of photographs illustrating examples of 1, 2, 3 and 5 drop arrays (and their reflections) of *n*-heptane, each drop being of volume 0.013 ml and at centre-to-centre spacings of 6 mm. The surface temperature was 250 °C. In figure 5*a* the entire surface is in view, including the heads of the mounting bolts. Because of the highly diffuse lighting, the depressions in the surface are not clearly visible though reflections of droplets on the polished surface are. The impressions of the machining tool at the centre of the depressions can be seen as black dots in figure 5*b–d*.

The test-surface temperature was obtained by extrapolating the measurements of four 1 mm diameter stainless steel sheathed chromel–alumel thermocouples inserted into the surface as shown in figure 2. Extrapolated surface temperatures were found to be within 1 °C of the temperature recorded by the uppermost thermocouple (located 0.8 mm below the centre of the upper surface).

The test surface temperatures studied were below that at which spontaneous ignition would occur for the liquids studied (Tamura & Tanasawa 1959). Therefore, for experiments on droplet combustion, the droplets were ignited as they impacted the test surface by means of a spark from a Webster ignition transformer. The electrodes were made from 0.5 mm diameter stainless steel wire, with a 1 mm gap. The spark gap was located 5 mm above the surface, approximately 10 mm from the test-surface centre, and placed symmetrically with respect to the droplets in the array being studied. Evaporation of fuel from the droplets during formation at the ends of the injector tubes apparently created a pool of fuel vapour over the test surface. This was revealed by a large flame which engulfed nearly the entire array immediately after ignition (i.e. within 33 ms which was the minimum time between successive images in the video display). Figure 6, plate 3, shows this large flame engulfing an array of five drops of *n*-heptane (0.013 ml) at a centre-to-centre spacing of 6 mm on a surface at 250 °C. These stray fuel vapours were apparently consumed within less than 1 s (the time between photographs) after their ignition after which the flames ascended into the air above the droplets and assumed a relatively stable shape as shown in figure 7, plate 3.

Measurements of droplet evaporation time, droplet diameter and levitation height were made using a Video Logic CDR-460 video camera equipped with extension bellows and a 105 mm macro lens. The camera drove a General Radio Model 1538-A strobe which was the only source of illumination, providing 1 μs duration images at the rate of 30 per second thus eliminating any blurring due to droplet motion. A Vicon V240TW timer added a time display with a resolution of 0.1 s to the video image. Droplet diameter and levitation height measurements were made directly from the magnified image on an Audiotronics 13 in black and white monitor, using a scale with movable cross hairs (Colorado Video Caliper model 306). The resolution of the measurements was restricted by the dimensions of the pixels of the video screen, and was estimated to be about 0.007 mm at the magnification used. The camera was placed at a slight incline to the surface to coincide with the angle of the conical depression (2° to 4°, depending on the surface) to avoid obscuring the view of the bottom of the droplet placed in the depression. This inclination, however, gave the same measurements as a camera placed horizontally.

Droplets in Leidenfrost evaporation (e.g. figure 5) were photographed by a 35 mm Nikon F-3 camera with a 105 mm lens on Kodak Panatomic-X (32 ASA) film, with an f-stop of 32 to provide the maximum possible depth of focus. Highly diffused backlighting was provided by two Vivitar 285 electronic flash units set at maximum intensity, placed inside a 150 mm diameter white paper tube and held behind a ground glass diffuser mounted 50 mm from the centre of the test surface.

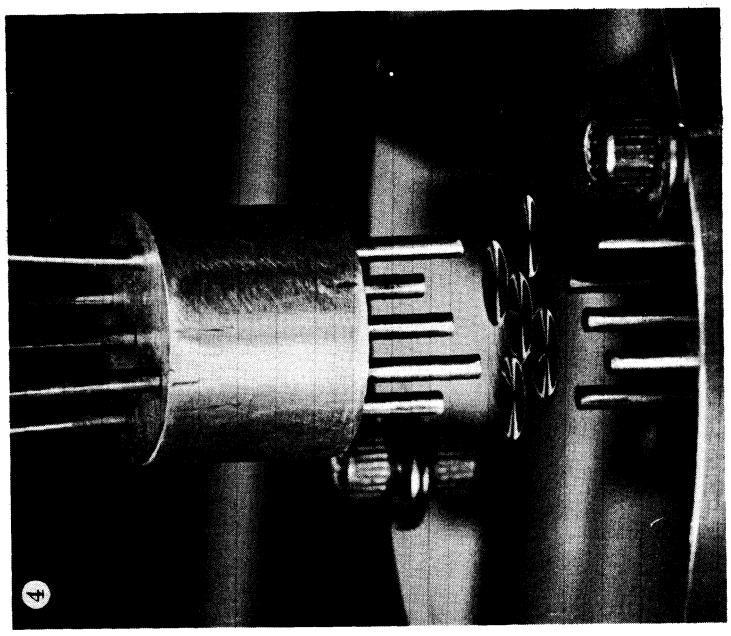

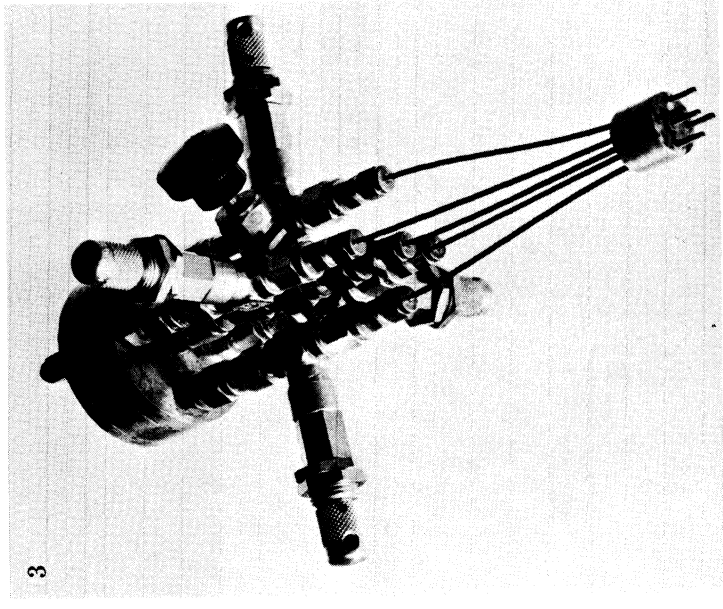

FIGURE 3. Droplet generator.

FIGURE 4. Droplet generator tubes positioned above test surface with five depressions.

(*Facing p.* 370)

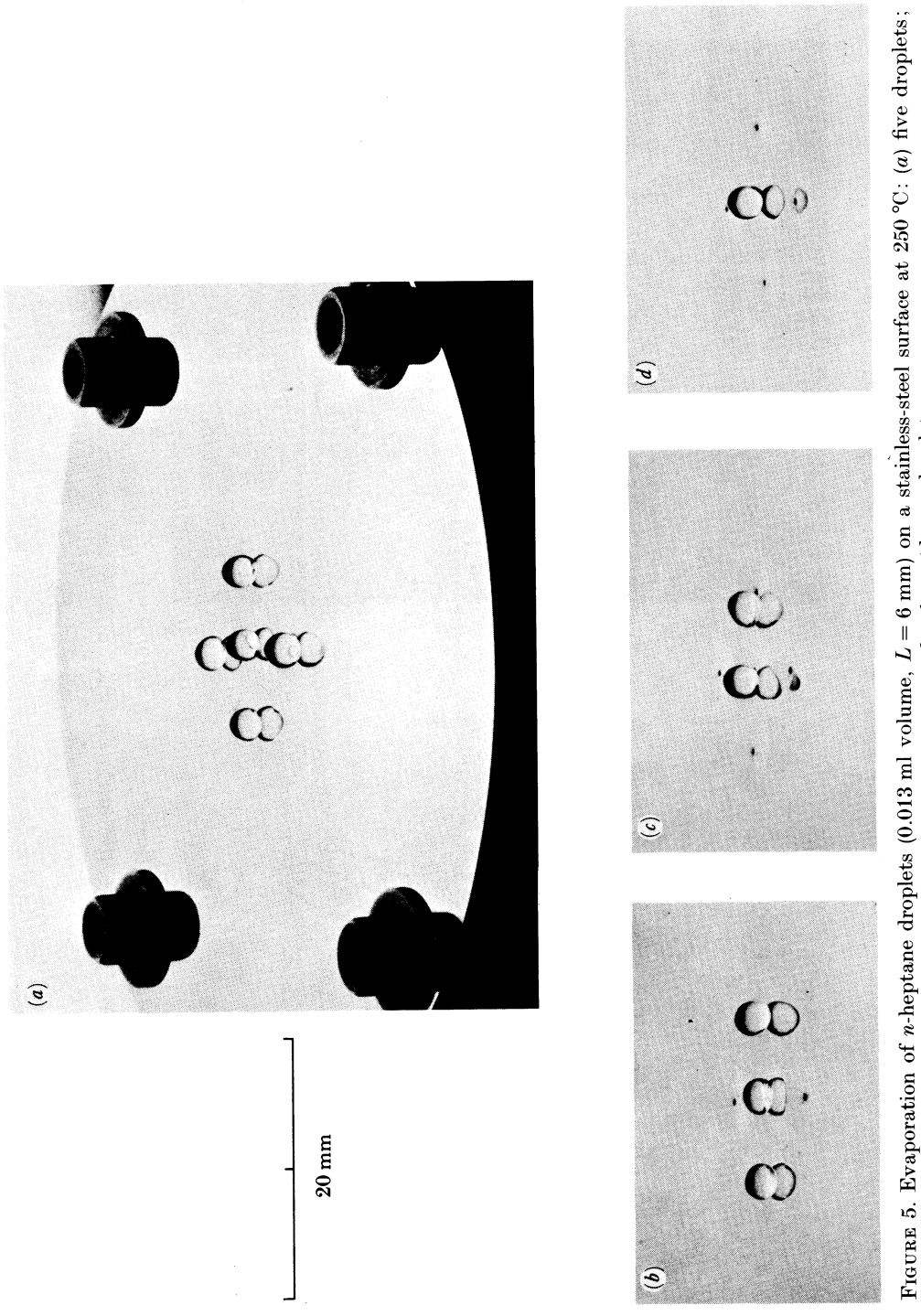

FIGURE 5. Evaporation of *n*-heptane droplets (0.013 ml volume, $L = 6$ mm) on a stainless-steel surface at 250 °C: (*a*) five droplets; (*b*) three droplets; (*c*) two droplets; (*d*) one droplet.

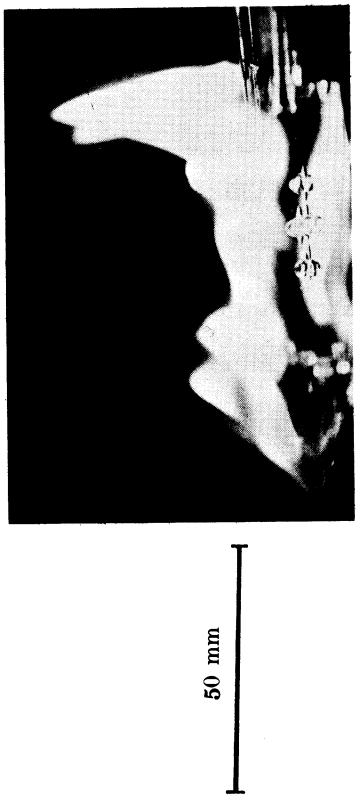

FIGURE 6. Ignition of a five-droplet array of *n*-heptane droplets (0.013 ml volume, $L = 6$ mm) on a stainless-steel surface at 250 °C ($t = 0$ s).

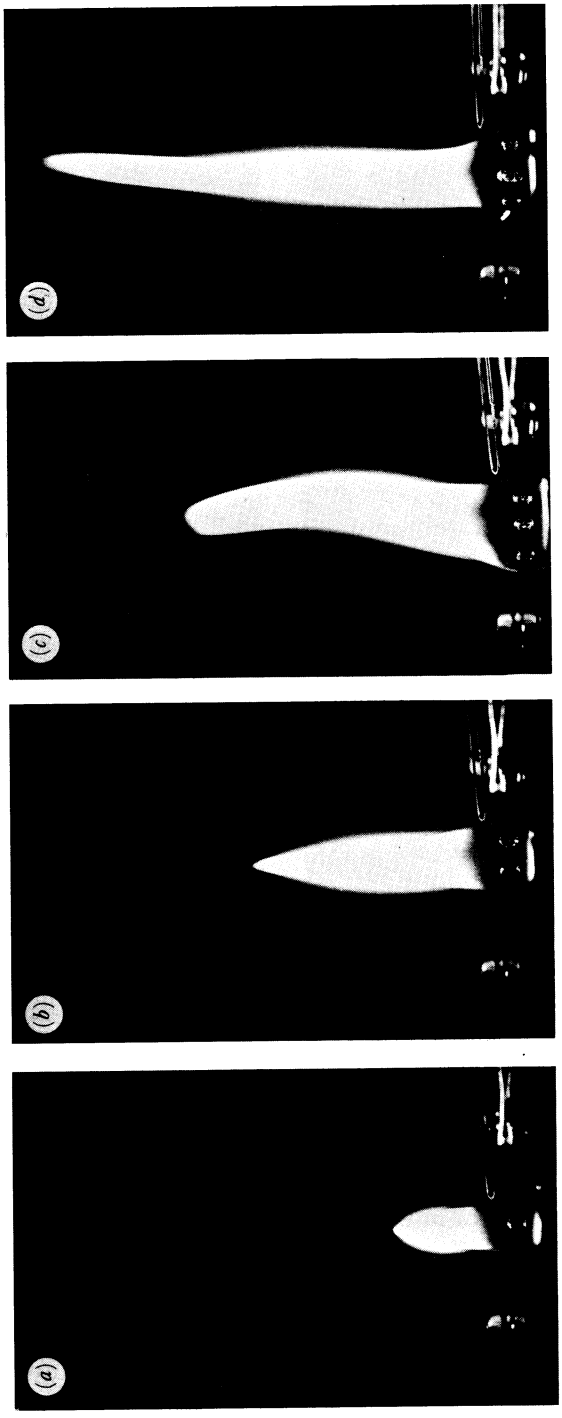

FIGURE 7. Combustion of *n*-heptane droplets (0.013 ml volume, $L = 6$ mm) on a stainless-steel surface at 250 °C ($t = 1$ s): (*a*) one droplet; (*b*) two droplets; (*c*) three droplets; (*d*) five droplets.

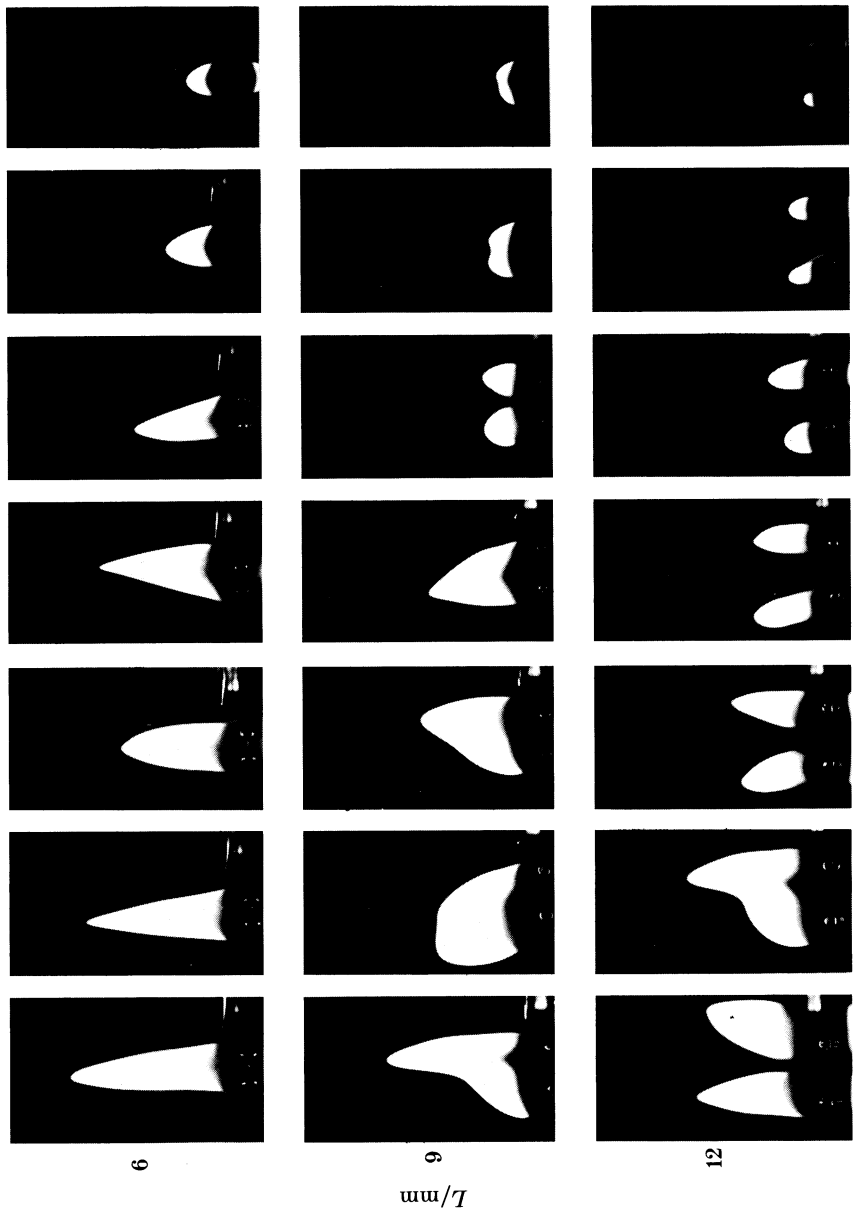

FIGURE 8. Combustion of *n*-heptane droplets (0.013 ml volume) on a stainless-steel surface at 250 °C.

Photographs of the flames surrounding the droplets were taken by the same camera and lens with Kodak Tri-X (400 ASA) film. The film was advanced at a rate of one frame per second by a Nikon MD4 motordrive unit driven by a pulse generator. Lighting was obtained solely from the luminosity of the flame. For all flames photographed a shutter speed of $\frac{1}{30}$ s and an aperture of f-4 was used. Figures 6 and 7 and figure 8, plate 4, show examples of photographs of flame geometry made by this method.

The droplets exhibited a slight flattening under their own weight as they rested on a cushion of vapour. An equivalent droplet diameter was therefore defined by assuming the droplet to be a volume of revolution about the vertical axis, with an elliptic cross section. The equivalent diameter (d) was calculated as

$$d = (a^2 b)^{\frac{1}{3}},$$

where a and b were the horizontal and vertical droplet axes. These dimensions were measured at each instant from a single frontal video image by the video caliper. To verify the accuracy of the assumption that the droplet was a volume of revolution, simultaneous photographs of a single drop in Leidenfrost evaporation were taken by two cameras placed along perpendicular lines of vision. Equivalent droplet diameters calculated from these two views of the same droplet differed by an average of about 3%.

3. Discussion

3.1. *Binary droplet arrays*

Binary droplet arrays did not reveal any interactive effects on the evaporation and burning times (i.e. the time for complete disappearance of the droplets). This is illustrated in figure 9 for water and figures 10 and 11 for n-heptane and n-hexadecane respectively. Each data point in these figures represents an average of ten observations, the lines drawn through the data in these and all remaining figures are curves of best fit. The evaporation or combustion time of the two droplets in a binary array differed at most by 3%. The indicated Leidenfrost temperatures are consistent with prior observations of isolated droplets (Gottfried & Bell 1966; Tamura & Tanasawa 1959); the Leidenfrost temperatures for droplets in the binary arrays were the same as those of isolated droplets for $6\text{ mm} < L < \infty$. Flame interactions (see figure 8) also were apparently not sufficient to affect the burning rate even when such an influence might have been expected based on prior experiments for binary droplet arrays in an *unbounded* ambience (Rex *et al.* 1956; Fedoseeva 1972; Miyasaka & Law 1981).

The critical spacing for flame mergence around arrays of two n-heptane droplets was at $L/d_0 \approx 4$. This value is close to that reported by Brzustowski *et al.* (1979) for suspended binary n-heptane droplet arrays: $L/d_0 \gtrsim 3$. This slight increase in critical spacing for flame mergence in Leidenfrost combustion compared to combustion far from a surface is caused by the greater width of the flame around a droplet burning at the surface. The flame does not extend around the underside of the droplet but is instead spread out by the fuel vapours venting from the vapour film which exists between the droplet and the test surface. For a given

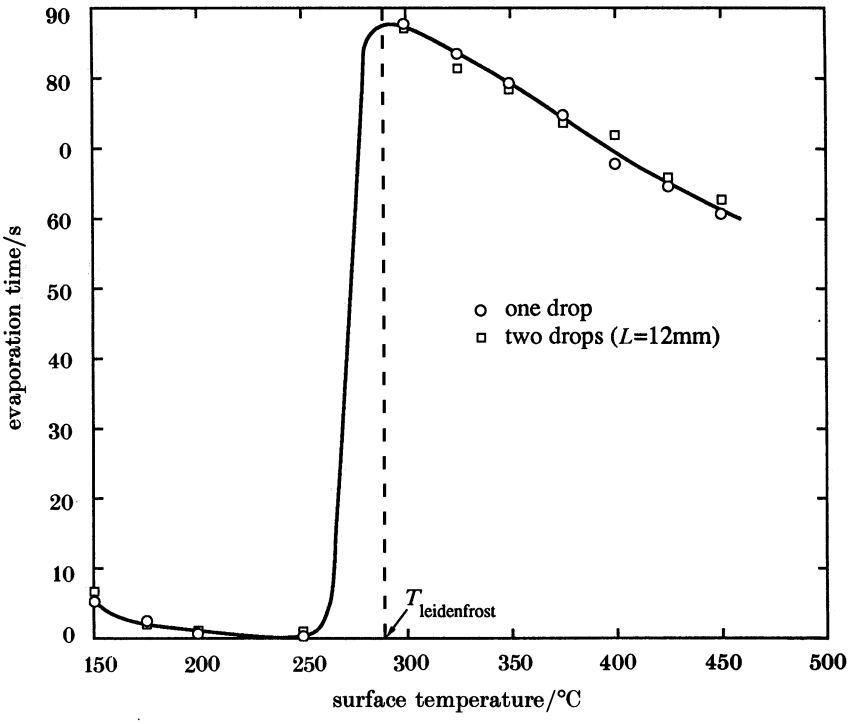

FIGURE 9. Variation of evaporation time with surface temperature for water drops (0.031 ml volume) on a stainless-steel surface.

droplet diameter the flames are thus wider for droplets in Leidenfrost evaporation than for droplets in an unbounded ambience where the flame extends around the entire circumference of the droplet. Mergence then occurs at a larger interdroplet spacing than for droplets in an unbounded ambience. The flame height, though, was found to be dependent on droplet separation distance for binary arrays as shown in figure 8. As L was reduced from 12 mm to 9 mm, the flame height H increased by 20%, and at $L = 6$ mm by 35%. This height difference, though, had no apparent effect on the evaporation or burning rate.

Figure 12 illustrates the variation of droplet combustion time with the centre-to-centre distance at several surface temperatures for n-heptane (figure 12a) and n-hexadecane (figure 12b), in the range $6\text{ mm} < L < \infty$ and at three surface temperatures. The bars shown represent the maximum and minimum measured combustion times for an averaged ten observations at each spacing. Any variation of combustion time with spacing is seen to be less than the scatter of the data. Therefore, within the sensitivity of the experimental measurements, no influence of droplet separation distance on droplet combustion rates was found.

The absence of interactions in binary arrays is further illustrated by the evolution of droplet diameter shown in fig. 13 for $L/d_0 \approx 2$ (the closest spacing studied) and a surface temperature of 250 °C. The data in figure 13 follow an evolution law of the form

$$d^n = d_0^n - kt, \tag{1}$$

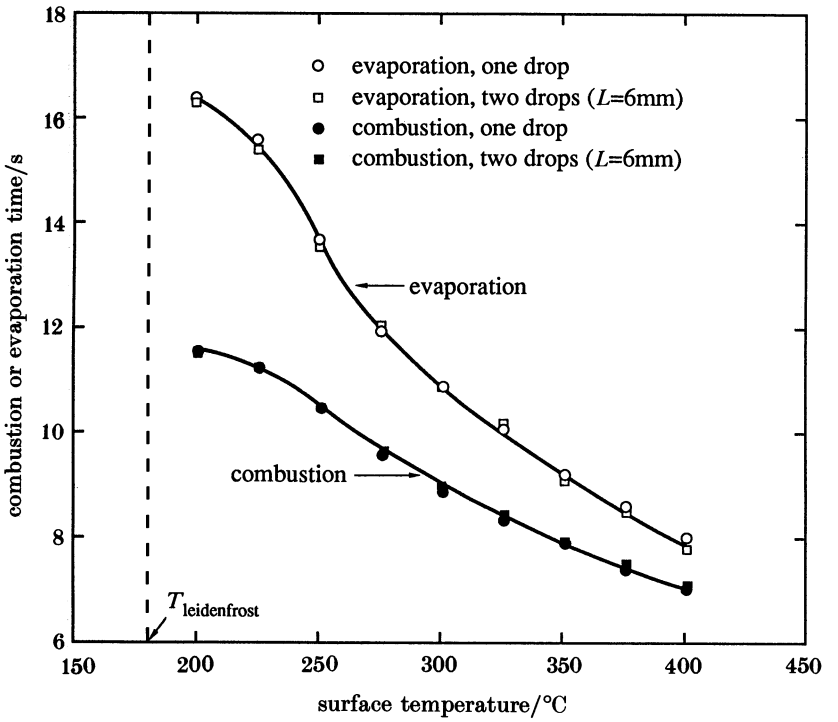

FIGURE 10. Variation of evaporation or combustion time with surface temperature for *n*-heptane drops (0.013 ml volume) on a stainless-steel surface.

where $n = 1.25$ for an isolated Leidenfrost droplet (Satcunanathan 1968). It is seen that this law also represents quite well the evaporative–burning history of a binary array. As such, any effects of interdroplet spacing do not apparently extend to the evolution of droplet diameter.

As an additional point in connection with figure 13, the data for complete evaporation or combustion (see figures 9–11) were taken from the video record to correspond to the instant when the droplet could no longer be seen. Close examination of images at large magnification ($\times 50$) showed that droplets sometimes collapsed on the surface before complete evaporation. Extrapolation of diameter–time data showed that this effect could lead to underestimating the evaporation time by less than only 1%. The reason for impact with the surface just before complete disappearance is most likely that there are small amounts of impurities ($< 1\%$) in liquids certified to be even 99% pure.

The failure to observe experimentally any interaction between two droplets in Leidenfrost evaporation is in contrast to previous studies which have demonstrated significant interactive effects, most notably a reduction in droplet evaporation rate, for droplets in an *unbounded* ambience (i.e. far from walls). A possible explanation for an absence of discernible interactions may reside in the dominance of heat transfer to the droplet from the test surface over gas phase heat transfer from the flame. Estimates of the gas phase and surface heat transfer rates are given below.

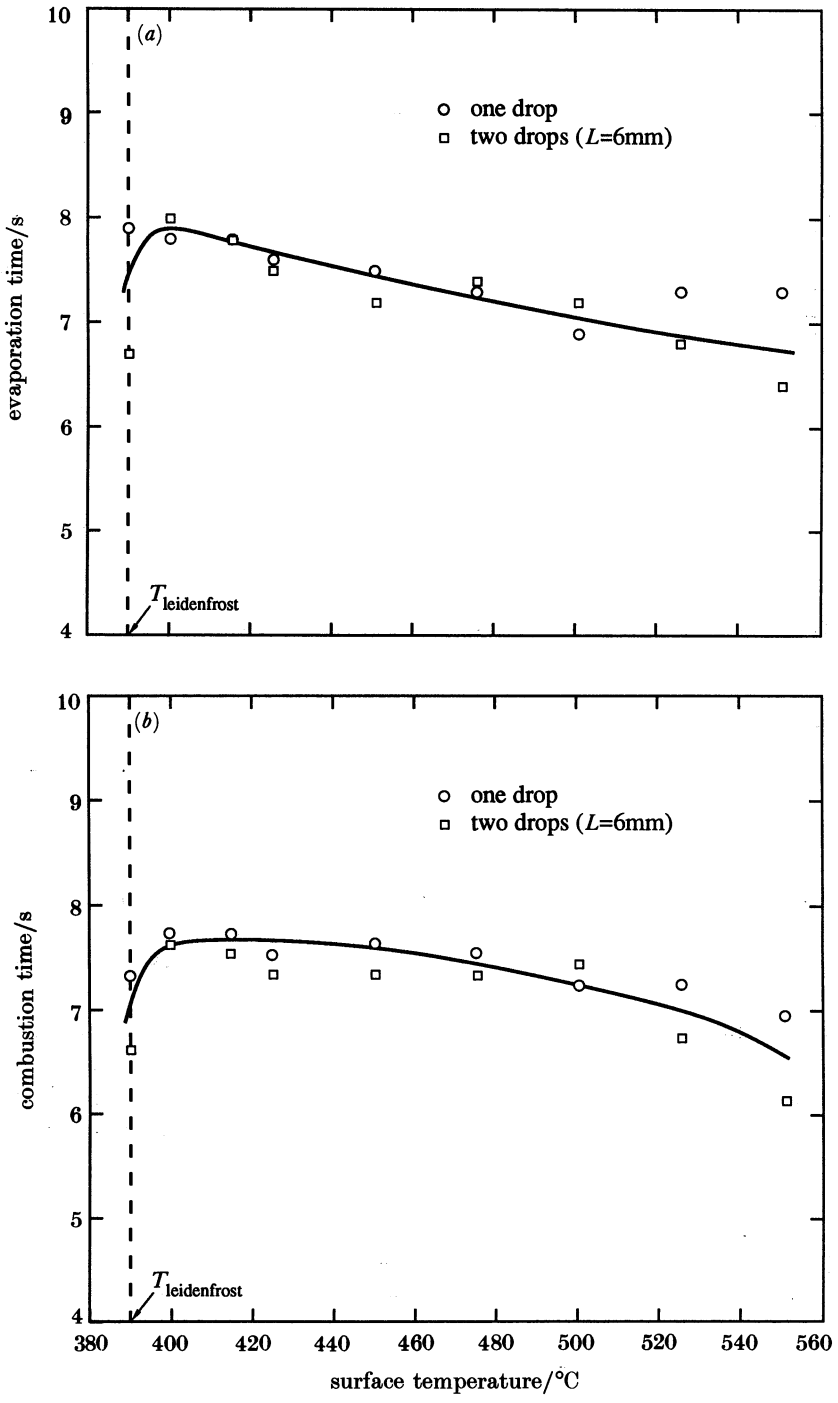

FIGURE 11. (*a*) Variation of evaporation time with surface temperature for *n*-hexadecane drops (0.015 ml volume) on a stainless-steel surface. *b*. Variation of combustion time with surface temperature for *n*-hexadecane drops (0.015 ml volume) on a stainless-steel surface.

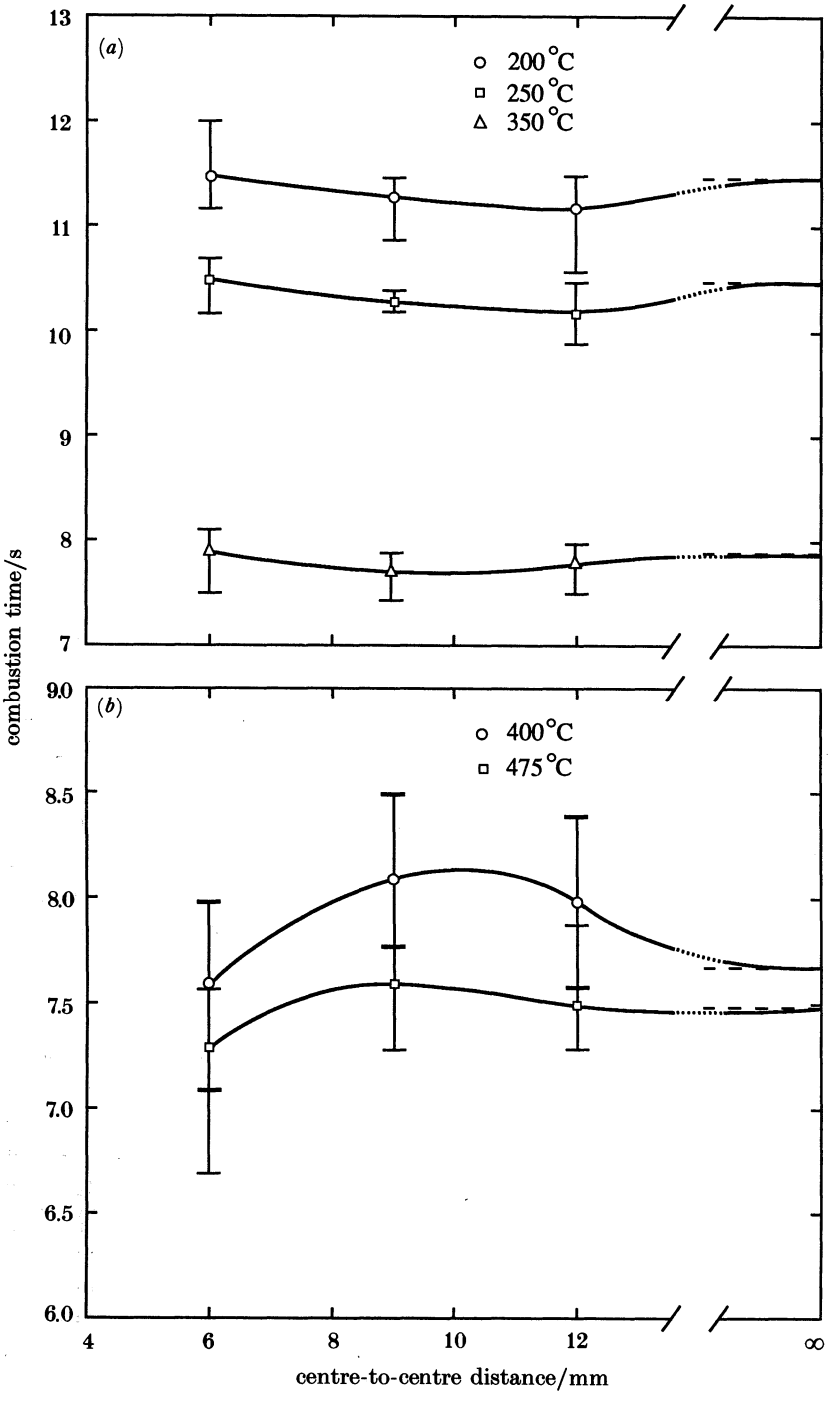

FIGURE 12. (*a*) Variation of combustion time with centre-to-centre distance for *n*-heptane drops (0.013 ml volume) on a stainless-steel surface. (*b*) Variation of combustion time with centre-to-centre distance for *n*-hexadecane drops (0.015 ml volume) on a stainless-steel surface.

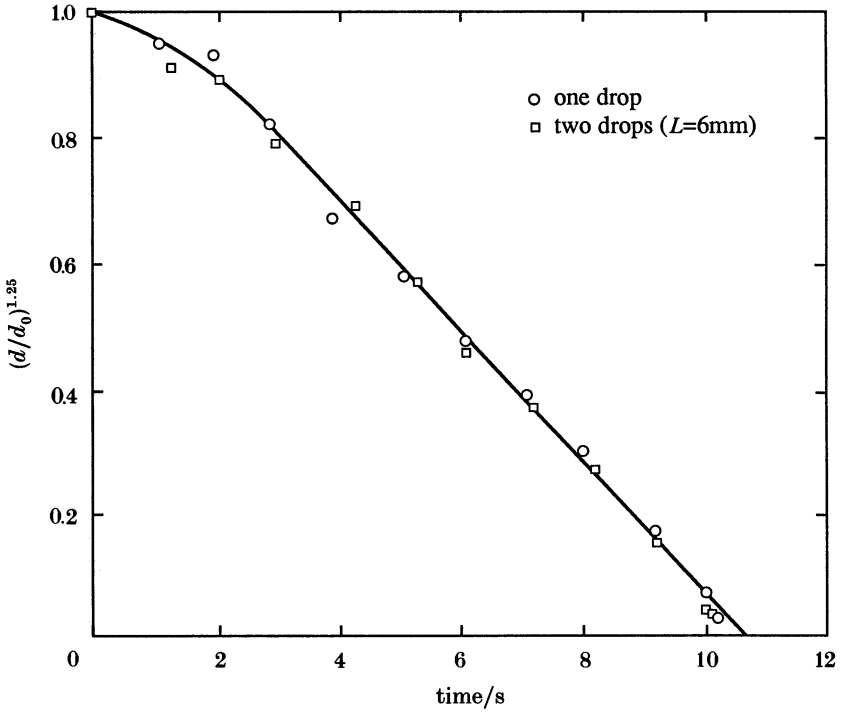

FIGURE 13. Variation of droplet diameter with time for combustion of one drop and two drop arrays of n-heptane (0.013 ml volume) on a stainless-steel surface at 250 °C.

Heat transfer from the hot surface to the underside of the droplet may be modelled by simple conduction across the thin vapour film of thickness δ (being of the order of 0.002 cm at the start of burning based on our photographic observations), which separates the droplet from the surface. This heat flux is approximately

$$q_w \sim k_g(T_w - T_d)/\delta. \tag{2}$$

The gas-phase heat transfer to the droplet was considered to have two contributions: one owing to convection originating from the flame which creates a buoyancy induced gas flow around the edge droplet in the array the magnitude of which is a function of the flame height, and hence number of droplets in the array; one from radiative heat transfer from the flame to the edge droplet. Radiative heat transfer from the flame, being modelled as $q_{rad} \sim \sigma F_{df}(T_f^4 - T_d^4)$, was found to be nearly constant with respect to changes in flame height. The radiation shape factor between the flame and the droplet, F_{df}, was approximated by the shape factor between a sphere and rectangle perpendicular to the line through the sphere axis (Howell 1982, p. 190). This shape factor exhibited a weak dependence on flame height H_i (i.e. the length of the rectangular edge) for the range of heights measured in these experiments (25 mm $< H_i <$ 120 mm, where i is the number of droplets in the array). As a result the radiative contribution to the total gas phase heat transfer rate to the edge droplet in the array was considered to be

independent of the number of droplets in the array. By contrast the convective heat flux contribution, modelled as

$$q_{fi} \sim k_g[(T_f - T_d)/d]Nu_i \tag{3}$$

exhibited a much stronger dependence on flame height, changing by over 20% for the range of measured flame heights. The effect of adding more droplets to the array on the gas-phase heat-transfer rate to the edge droplets was thus considered to be carried entirely in the convective contribution, with the radiative transfer being effectively independent of the number of droplets.

The Nusselt number was related to flame height through the buoyancy induced gas velocity. An order of magnitude for this velocity was obtained by balancing the buoyancy and viscous terms in the momentum equation to yield

$$u_i \sim (g\beta\Delta T H_i)^{\frac{1}{2}} \tag{4}$$

With this characteristic velocity and a Nusselt number based on the classical Ranz-Marshall (1952) form we have that

$$Nu_i \equiv hd/k_g = 2 + CH_i^{\frac{1}{4}}, \tag{5a}$$

where

$$C \equiv 0.6Pr^{\frac{1}{3}}[(g\beta\Delta T)^{\frac{1}{2}}d/\nu]^{\frac{1}{2}}. \tag{5b}$$

Taking $\delta \sim 0.002$ cm, $d \sim 3$ mm, $T_w \sim 250$ °C, $T_d \sim 100$ °C, $T_a \sim 25$ °C, $T_f \sim 2000$ °C, $k_g = 8.2 \times 10^{-4}$ W cm^{-1} K^{-1}, $\nu \sim 1.8$ cm^2 s^{-1}, $\beta \sim 7.7 \times 10^{-4}$ K^{-1}, $H_1 \sim 2.63$ cm (measured), and $Pr \sim 1$, we have for one droplet that $q_{f1}/q_w \sim 0.34$ and $q_{rad}/q_w \sim 0.32$. The presence of a second droplet was found to increase flame height by a factor of about two (figure 7), but q_f by a factor of only about 1.1 and q_{rad} by 1.01. However, progressively adding more droplets to build up the array and thereby increasing H created more discernible changes in q_{fi} whereas q_{rad} was effectively unchanged from its value for a single droplet as discussed in §3.2. For pure evaporation $H = 0$ and $q_{fi} = q_{rad} = 0$.

In a binary array the flame height was significantly affected by the spacing between droplets. Figure 8 shows that as two droplets are brought closer together not only do the flames merge but the flame height increases. This also suggests more significant interactive effects caused by adding more droplets to the array with a possible consequent increase in gas-phase heat transfer from the flame to the droplet due to increased flame heights.

To examine whether or not higher-order arrays produced more significant effects on droplet burning rates, arrays of three and five droplets were studied in the configurations shown in figure 1.

3.3. *Three- and five-droplet arrays*

Figure 14 shows the evolution of flame height for several different arrays of *n*-heptane droplets at a centre-to-centre spacing of 6 mm on a surface at 250 °C. Other surface temperatures yielded the same qualitative trends. For the data shown in figure 14 a single flame surrounded the entire array. It may be mentioned that at the moment of ignition ($t = 0$) it was not possible to define a flame height owing to the combustion of fuel vapours surrounding the droplets (see figure 6). All flame height measurements were therefore made starting at $t = 1$ s, by which time

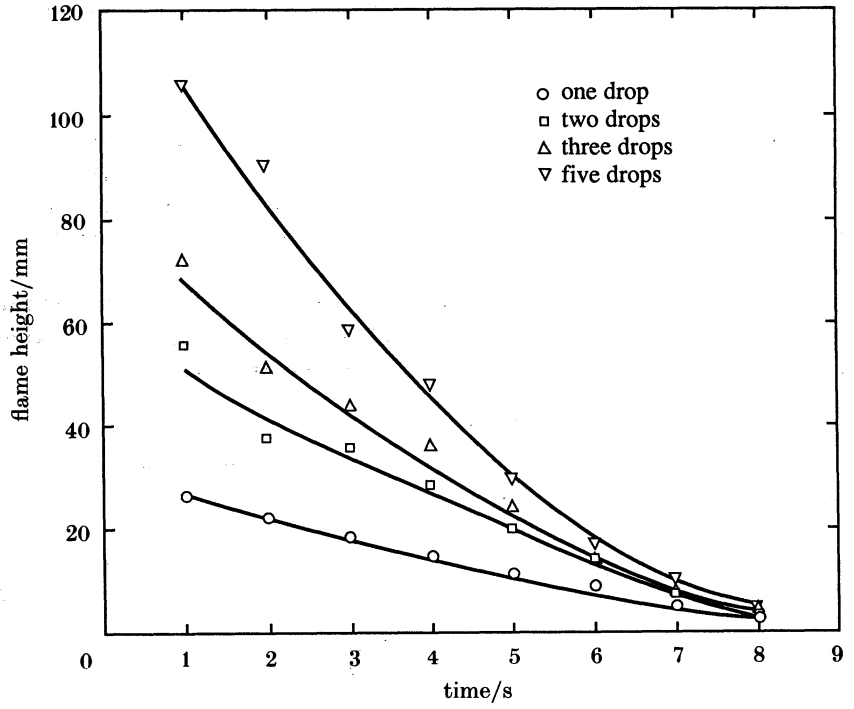

FIGURE 14. Variation of flame height with time for arrays of n-heptane droplets. (0.013 ml volume, $L = 6$ mm) on a stainless-steel surface at 250 °C.

the flame had assumed a relatively stable shape whose height could be measured with a repeatability of $\pm 10\%$.

At any given time in the evaporative history, the flame height increased as more droplets were added to the array. This increase, revealed in the measurements displayed in figure 14, is clearly shown in figure 7 for a single droplet (a) and arrays of two, three and five droplets (b, c, and d respectively) at a surface temperature of 250 °C. The effect of this progressive increase in flame height with number of droplets is to increase the gas-phase heat transfer to the droplets in the array relative to heat transfer from the test surface.

Figure 15 illustrates the increased contribution of gas phase heat transfer to the edge droplet in an array of burning droplets the variation being dominated by the convective contribution q_{fi} in (3), as more droplets are added. The calculation is based on (2)–(5) ($q_{ti} = q_{fi} + q_w + q_{rad}$ in figure 15) and the flame height data illustrated in figure 14 at $t = 1$ s. The surface temperature was fixed at 250 °C for these calculations for illustration. q_{fi} increases by about 3% to 5% for three- and five-droplet arrays respectively. This increase yielded a concomitant decrease in the total burning time by nearly the same amount at 250 °C as shown in figs. 16 and 17 for the edge droplets in three- and five-droplet arrays, respectively. This decrease, though small, was still larger than the standard deviation of 0.1 s for the burning-time data shown in these figures, particularly figure 17. By contrast, differences between the burning times of droplets 6 mm apart in a binary array

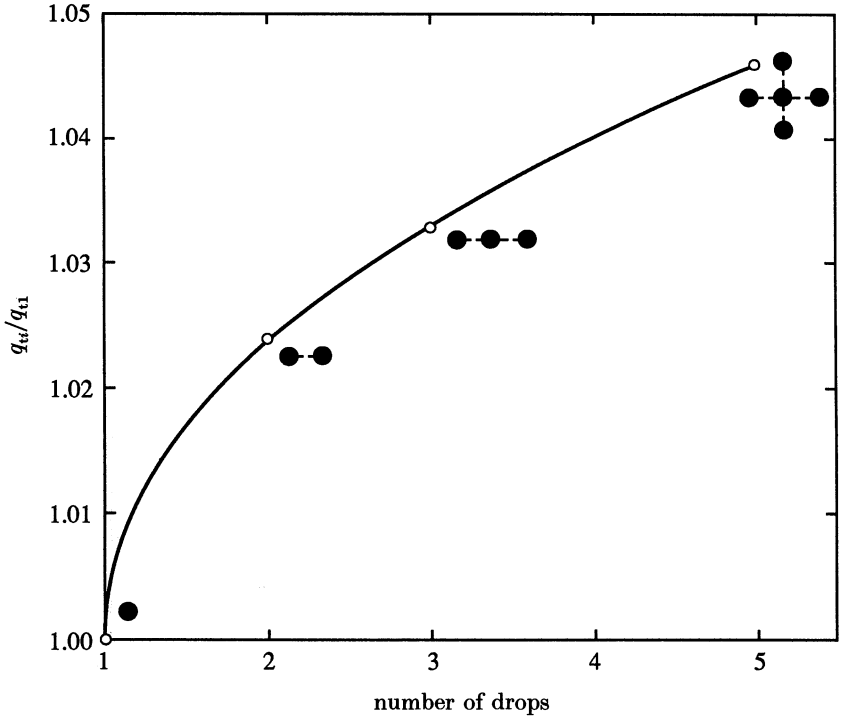

FIGURE 15. Variation of the total heat flux to a drop with the number of drops in the array for *n*-heptane drops (0.013 ml volume, $L = 6$ mm) on a stainless-steel surface at 250 °C.

were not detectable as discussed in §3.1. For pure evaporation (i.e. no combustion) the effect of neighbouring droplets on the evaporation rate was negligible even in a five-droplet array as shown in figures 16 and 17 because essentially all of the heat for evaporation comes from the test surface.

All the droplets in a three-drop array had a burning rate greater than that of a single drop because of the effect of buoyancy induced convective flows around the droplet. The centre droplet, however, shielded from the flame on both sides, burned slower than the edge droplets. Above a surface temperature of 250 °C, the heat flux from the surface q_w dominated heat transfer to the droplet, and changes in the convective contribution q_{fi} were no longer detectable.

Droplet interactions during combustion were most distinct for arrays of five droplets. Figure 17 shows evaporation or combustion times of the centre and edge droplets for such an array with centre spacings of 6 mm. For surface temperatures below 250 °C, the edge droplet in the array, which feels the effect of convective flows over it, apparently burns slightly faster than it would have had it stood alone (i.e. $L \rightarrow \infty$). The centre drop which is surrounded on all sides, burns slower than an isolated drop. This observation was clear from the video record from which it was seen that the centre droplet continued burning after the edge droplets in the array had disappeared. This difference was measurable until a surface temperature of about 375 °C was reached, above which heat transfer from the surface dominated any gas phase interactions present.

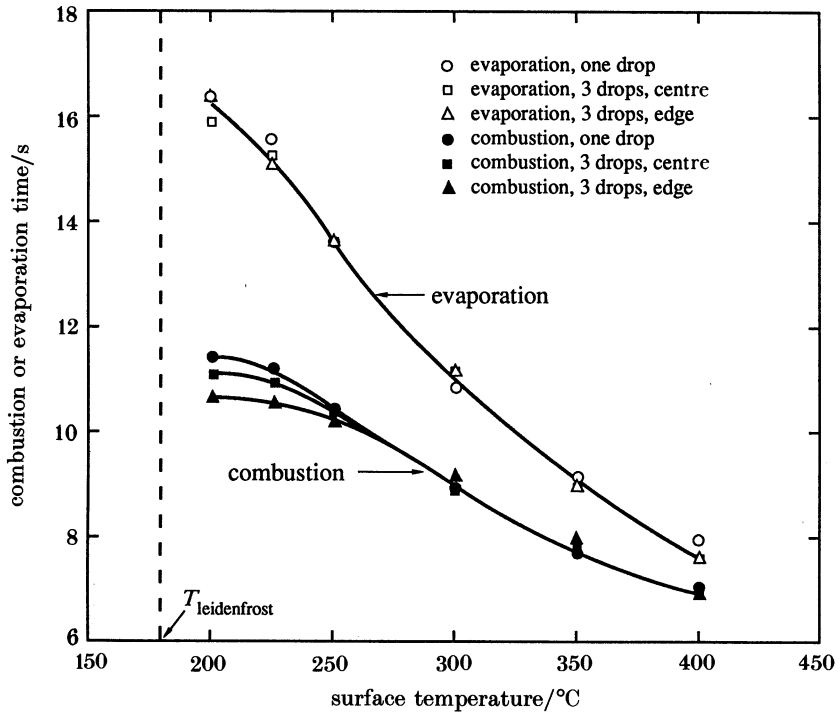

FIGURE 16. Variation of evaporation or combustion time with surface temperature for single drops and three drop arrays of *n*-heptane (0.013 ml volume, $L = 6$ mm).

Differences between combustion *rates* for centre and edge droplets in a five-droplet array are shown in figure 18. The surface temperature was fixed at 250 °C and the fluid was *n*-heptane. The slopes of the lines through the two sets of data are a measure of the burning rates and differ by about 20 %. The combustion rates of both centre and edge droplets show an increase near the end of their burning history. As the droplet size decreases, the flame surrounding the entire array separates and collapses around each droplet, thereby moving closer to them than when a single flame surrounds the entire array. The burning rate correspondingly increases as observed.

It should be noted that interactions between droplets can also be manifested by variations in the temperature within the surface above which the droplets are evaporating. Each location on the surface (there being a maximum of five such locations in the present study) at which a droplet resides can act as a heat sink owing to energy absorbed by the droplet during its evaporation or burning. The surface will then be locally quenched, even if only momentarily, during evaporation. This reduction in surface temperature extends throughout the solid. The effect of this reduction is a complicated question whose answer will reside in detailed subsurface temperature measurements. It is unlikely, though, that the stainless steel surface used in the present experiments would be susceptible to significant quenching (Baumeister & Simon 1973). As such, the interaction effects considered may well be restricted to the gas phase above the surface as conjectured herein.

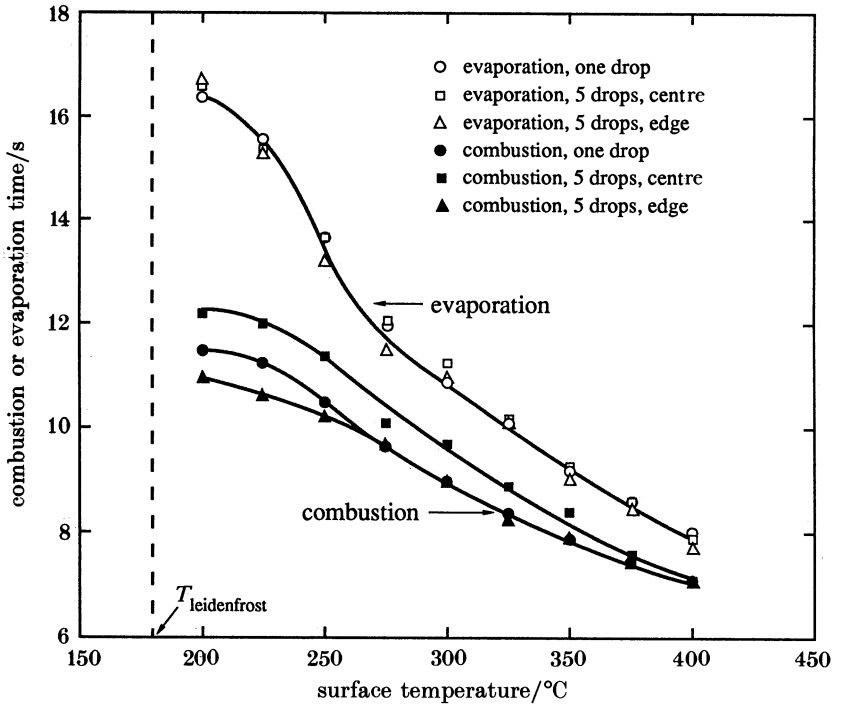

FIGURE 17. Variation of evaporation or combustion time with surface temperature for single drops and five-drop arrays of *n*-heptane (0.013 ml volume, $L = 6$ mm).

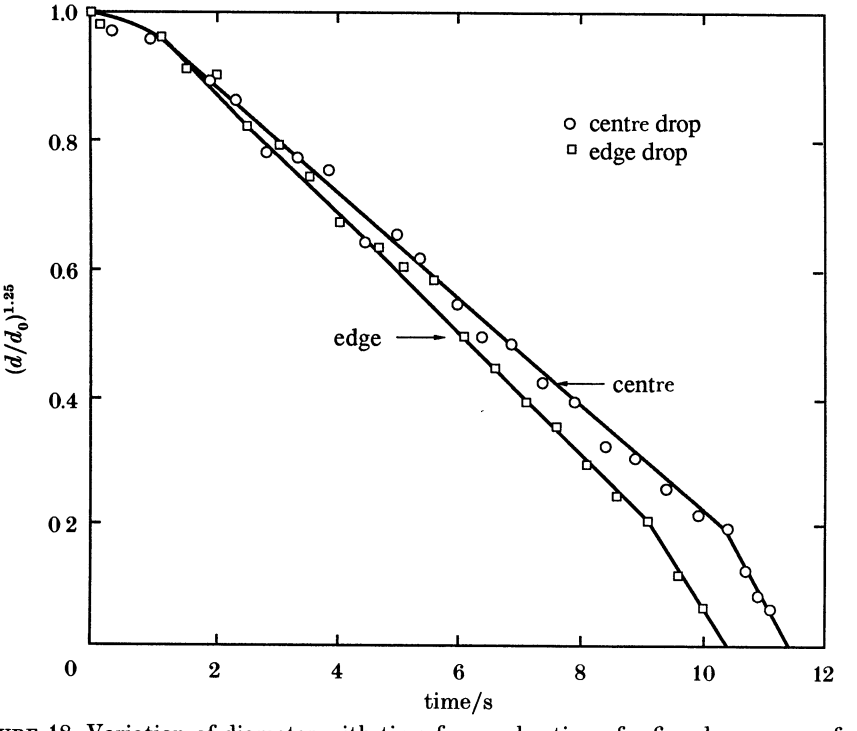

FIGURE 18. Variation of diameter with time for combustion of a five-drop array of *n*-heptane (0.013 ml volume, $L = 6$ mm) on a stainless-steel surface at 250 °C.

We thank Dr W. R. C. Phillips for reading the manuscript. This work was supported by the U.S. National Science Foundation through grant number CBT-8451075.

References

Avedisian, C. T. & Koplik, J. 1987 *Int. J. Heat Mass Transfer* **30**, 379–393.
Baumeister, K. J. & Simon, F. F. 1973 *J. Heat Transfer* **95**, 166–173.
Brzustowski, T. A., Twardus, E. M., Wojcicki, S. & Sobiesiak, A. 1979 *AIAAJl* **17**, 1234–1242.
Emmerson, G. S. 1975 *Inst. J. Heat Mass Transfer* **18**, 381–386.
Fedoseeva, N. V. 1972 *Adv. aerosol. Phys.* **2**, 110–119.
Gottfried, B. S. & Bell, K. J. 1966 *Ind. Engng Chem. Fundam.* **5**, 561–568.
Gottfried, B. S., Lee, C. J. & Bell, K. J. 1966 *Int. J. Heat Mass Transfer* **9**, 1167–1187.
Howell, J. R. 1982 *Radiation configuration factors*. New York: McGraw-Hill.
Miyasaka, K. and Law, C. K. 1981 In *18th Int. Symp. on Combustion*, pp. 283–292.
Ranz, W. E. and Marshall, W. R. 1952 *Chem. Engng Prog.* **48**, 173–180.
Rex, J. F., Fuhs, A. E. & Penner, S. S. 1956 *Jet Propulsion* **26**, 129–187.
Satcunanathan, S. 1968 *J. mech. Engng Sci.* **10**, 438–441.
Tamura, Z. & Tanasawa, Z. 1959 In *7th Int. Symp. on Combustion*, pp. 509–522. London: Butterworths.
Temple-Pediani, R. W. 1969–70 *Proc. Instn mech. Engrs* **184**, 677–696.
Xiong, T. Y., Law, C. K. & Miyasaka, K. 1984 In *20th Int. Symp. on Combustion*, pp. 1781–1787. Pittsburgh, Pennsylvania: The Combustion Institute.

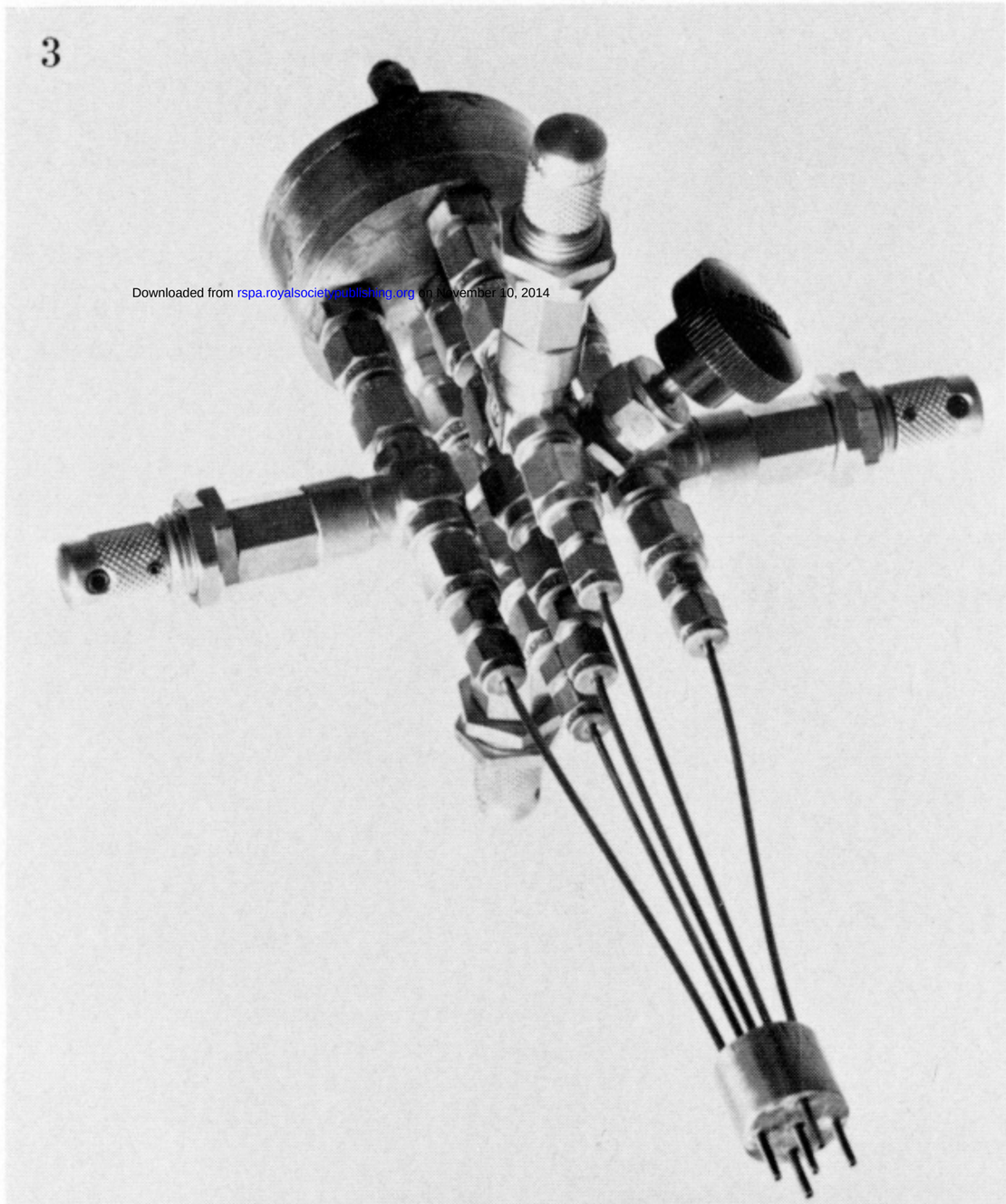

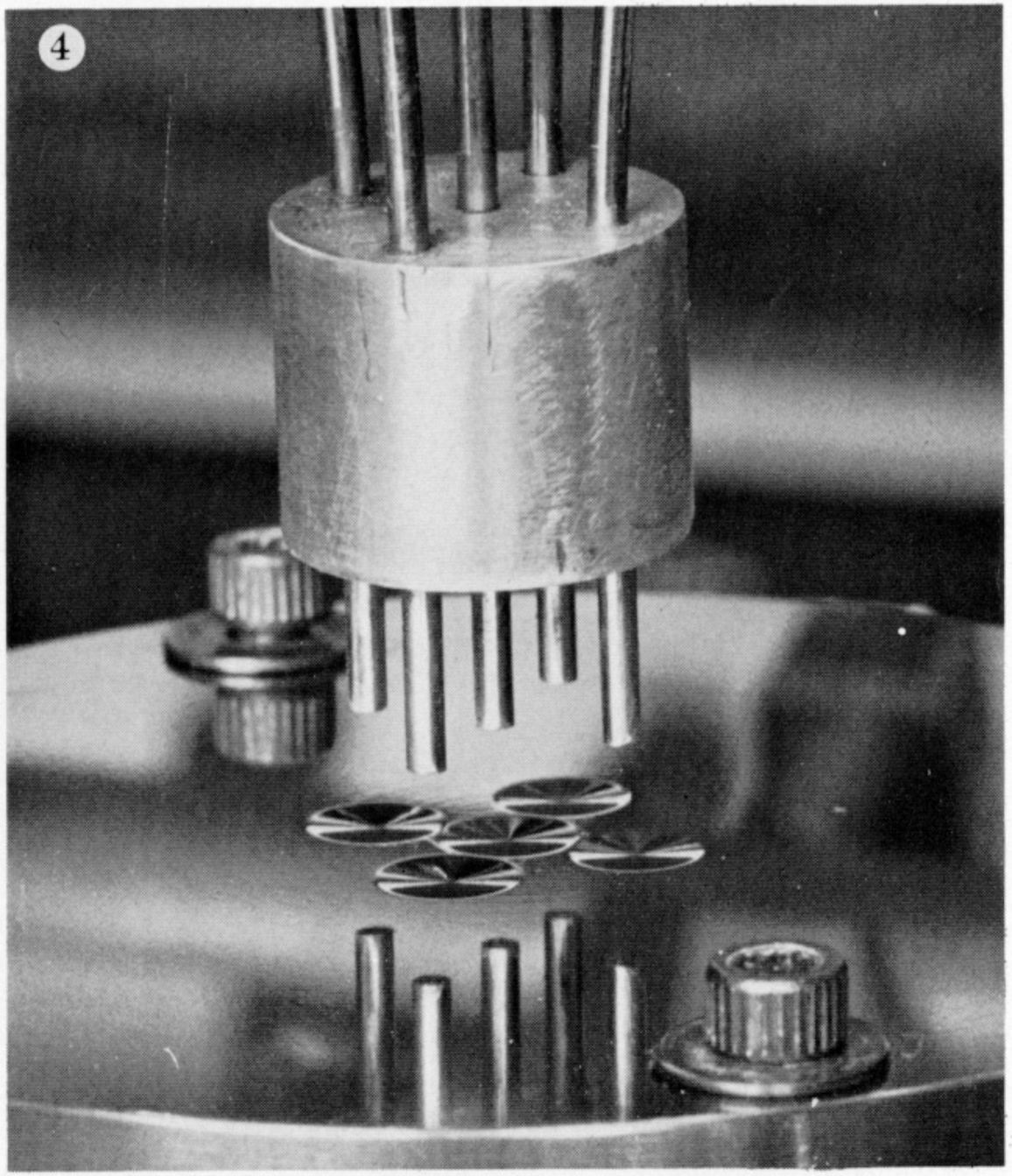

FIGURE 3. Droplet generator.

FIGURE 4. Droplet generator tubes positioned above test surface with five depressions.

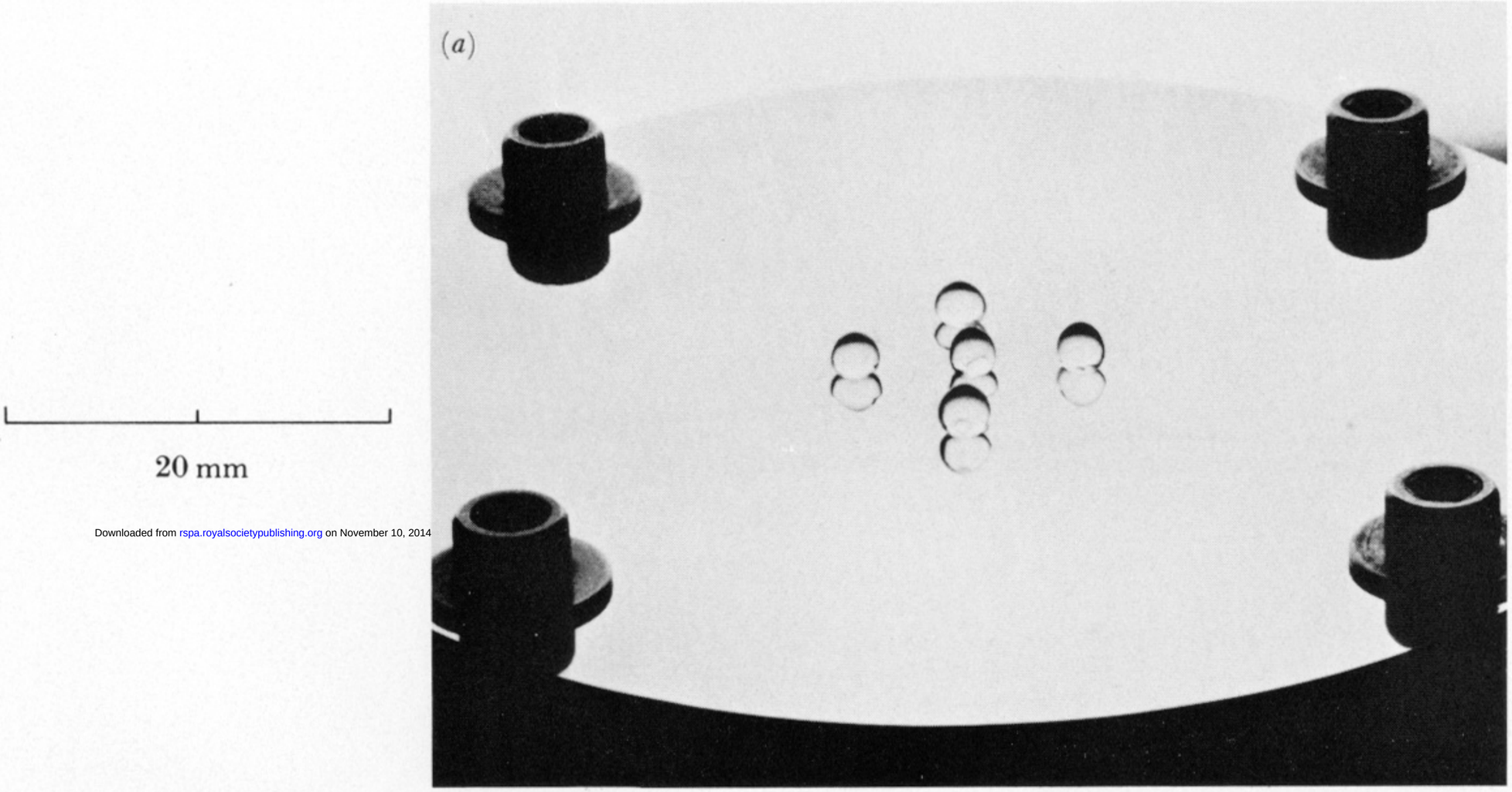

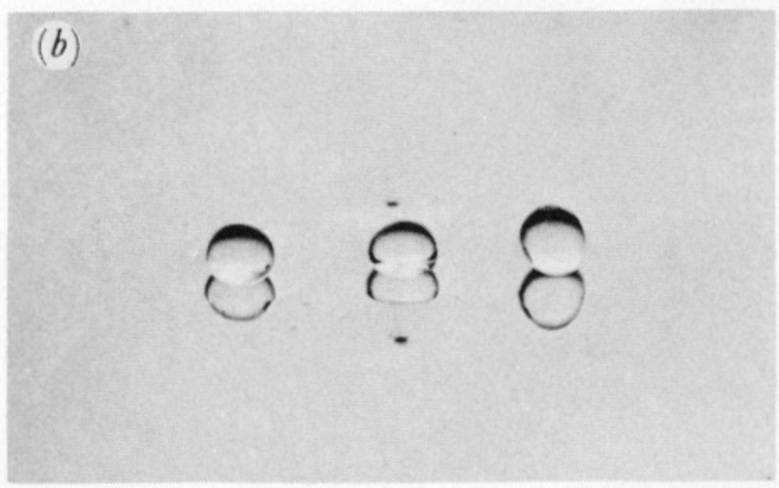

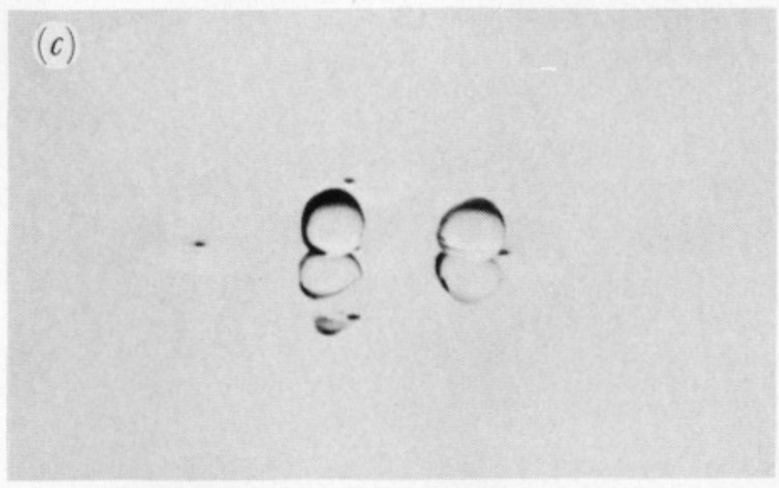

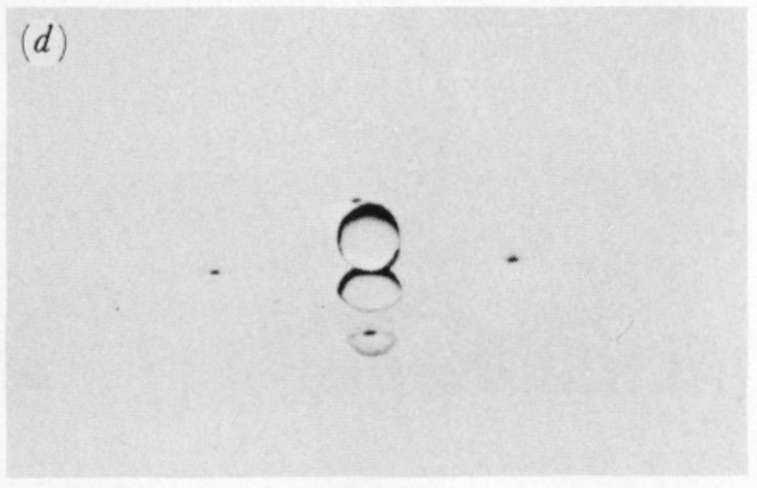

FIGURE 5. Evaporation of n-heptane droplets (0.013 ml volume, $L = 6$ mm) on a stainless-steel surface at 250 °C: (a) five droplets; (b) three droplets; (c) two droplets; (d) one droplet.

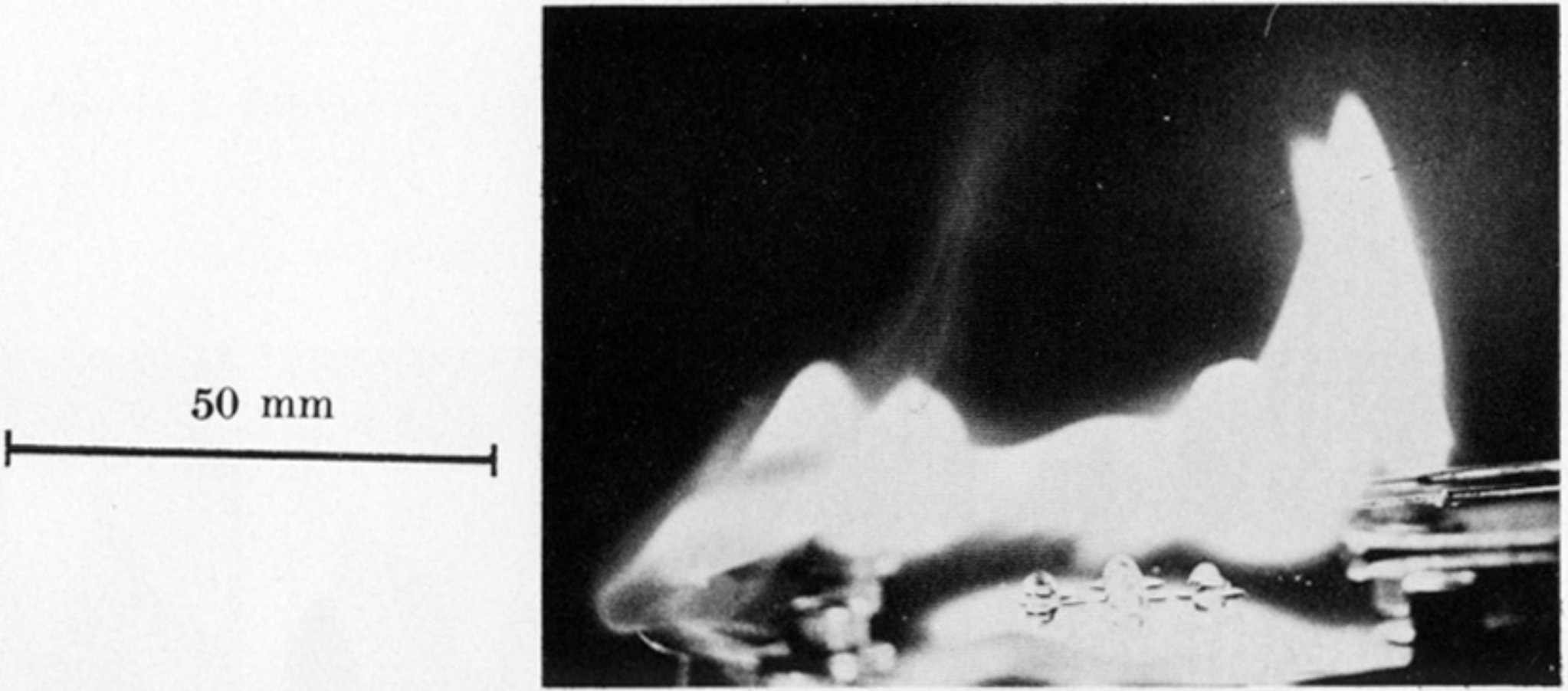

FIGURE 6. Ignition of a five-droplet array of n-heptane droplets (0.013 ml volume, $L = 6$ mm) on a stainless-steel surface at 250 °C ($t = 0$ s).

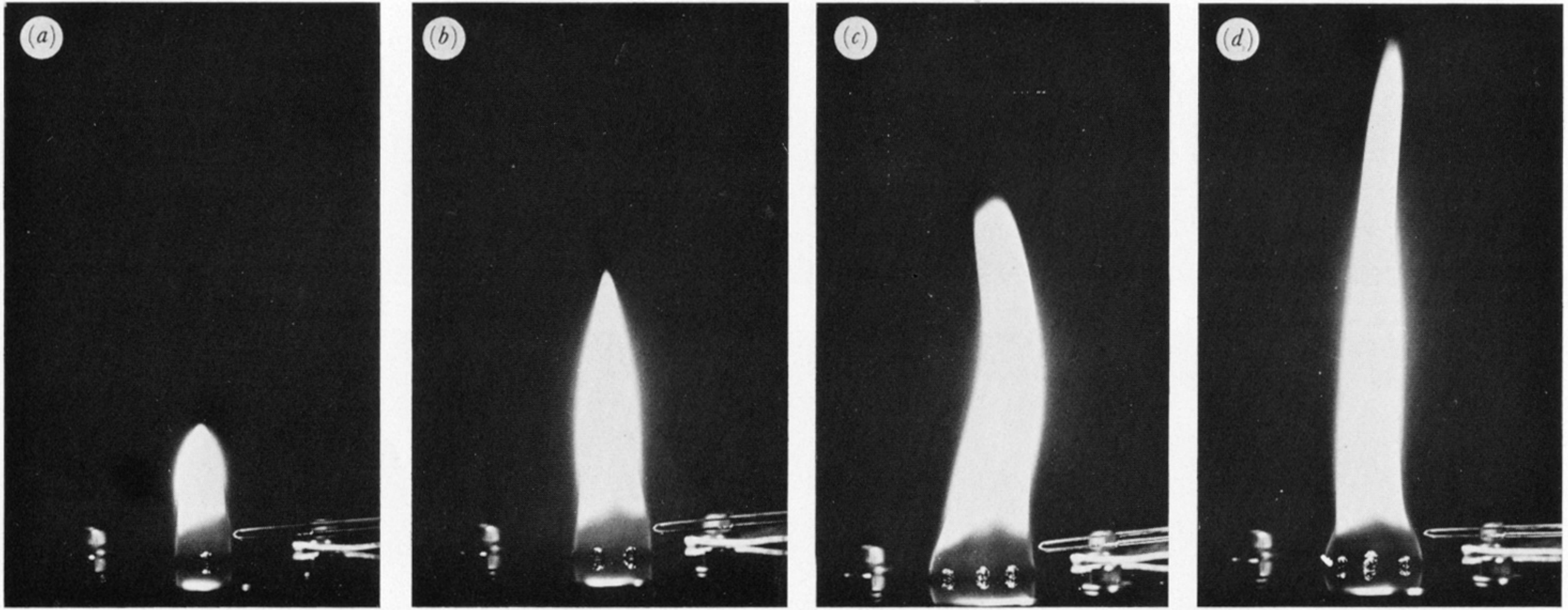

FIGURE 7. Combustion of n-heptane droplets (0.013 ml volume, $L = 6$ mm) on a stainless-steel surface at 250 °C ($t = 1$ s): (a) one droplet; (b) two droplets; (c) three droplets; (d) five droplets.

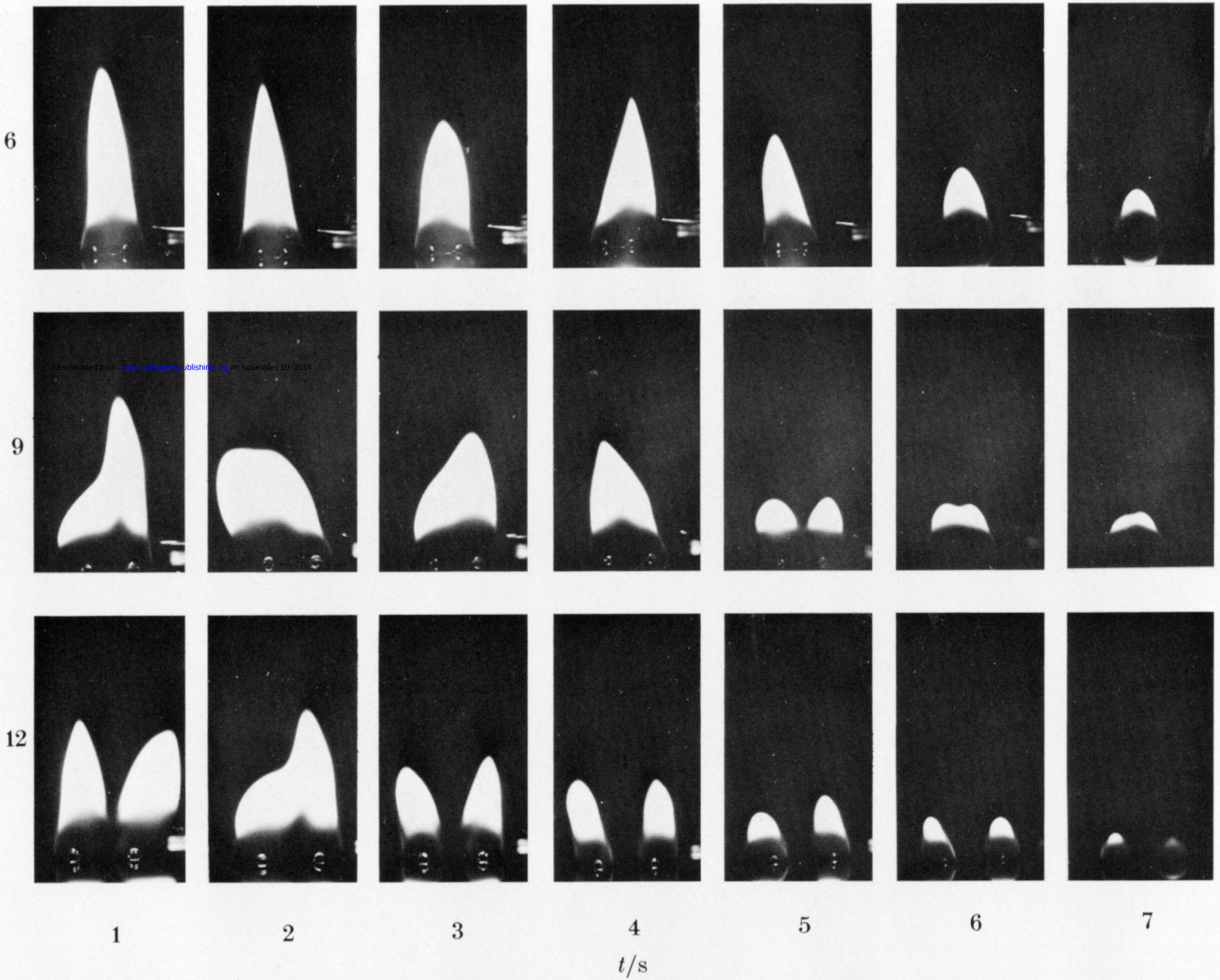

FIGURE 8. Combustion of *n*-heptane droplets (0.013 ml volume) on a stainless-steel surface at 250 °C.